



**HAL**  
open science

## Structure of the GTPase-binding domain of Sec5 and elucidation of its Ral binding site

Helen R Mott, Daniel Nietlispach, Louise J Hopkins, Gladys Mirey, Jacques H Camonis, Darerca Owen

► **To cite this version:**

Helen R Mott, Daniel Nietlispach, Louise J Hopkins, Gladys Mirey, Jacques H Camonis, et al.. Structure of the GTPase-binding domain of Sec5 and elucidation of its Ral binding site. *Journal of Biological Chemistry*, 2003, 278 (19), pp.17053-17059. 10.1074/jbc.M300155200 . hal-02683415

**HAL Id: hal-02683415**

**<https://hal.inrae.fr/hal-02683415>**

Submitted on 1 Jun 2020

**HAL** is a multi-disciplinary open access archive for the deposit and dissemination of scientific research documents, whether they are published or not. The documents may come from teaching and research institutions in France or abroad, or from public or private research centers.

L'archive ouverte pluridisciplinaire **HAL**, est destinée au dépôt et à la diffusion de documents scientifiques de niveau recherche, publiés ou non, émanant des établissements d'enseignement et de recherche français ou étrangers, des laboratoires publics ou privés.

Copyright

## Structure of the GTPase-binding Domain of Sec5 and Elucidation of its Ral Binding Site\*

Received for publication, January 7, 2003, and in revised form, March 6, 2003  
Published, JBC Papers in Press, March 6, 2003, DOI 10.1074/jbc.M300155200

Helen R. Mott<sup>‡</sup>, Daniel Nietlispach<sup>‡</sup>, Louise J. Hopkins<sup>‡</sup>, Gladys Mirey<sup>¶</sup>, Jacques H. Camonis<sup>¶</sup>,  
and Darerca Owen<sup>‡\*\*</sup>

From the <sup>‡</sup>Department of Biochemistry, University of Cambridge, 80, Tennis Court Road, Cambridge CB2 1GA, United Kingdom and the <sup>¶</sup>Institute Curie, 26, Rue d'Ulm, 75248 Paris Cedex 05, France

**The exocyst complex is involved in the final stages of exocytosis, when vesicles are targeted to the plasma membrane and dock. The regulation of exocytosis is vital for a number of processes, for example, cell polarity, embryogenesis, and neuronal growth formation. Regulation of the exocyst complex in mammals was recently shown to be dependent upon binding of the small G protein, Ral, to Sec5, a central component of the exocyst. This interaction is thought to be necessary for anchoring the exocyst to secretory vesicles. We have determined the structure of the Ral-binding domain of Sec5 and shown that it adopts a fold that has not been observed in a G protein effector before. This fold belongs to the immunoglobulin superfamily in a subclass known as IPT domains. We have mapped the Ral binding site on this domain and found that it overlaps with protein-protein interaction sites on other IPT domains but that it is completely different from the G protein-geranylgeranyl interaction face of the Ig-like domain of the Rho guanine nucleotide dissociation inhibitor. This mapping, along with available site-directed mutagenesis data, allows us to predict how Ral and Sec5 may interact.**

Spatial regulation of exocytosis is crucial for a variety of cellular processes, including embryogenesis, establishment and maintenance of cell polarity, and neuronal growth cone formation (reviewed in Ref. 1). The exocyst complex is involved in the final stage of exocytosis, when post-Golgi vesicles are targeted and dock to the plasma membrane. The exocyst consists of an assembly of eight proteins: Sec3, -5, -6, -8, -10, and 15, and Exo70 and -84, which form a complex localized to sites of vesicle docking to the plasma membrane during exocytosis.

In *Saccharomyces cerevisiae* the exocyst directs vectorial tar-

geting of secretory vesicles to sites of membrane expansion, such as bud sites. It appears that Sec3p, which is always localized to the plasma membrane, forms a targeting patch and is the spatial landmark for polarized exocytosis (reviewed in Ref. 1). A subcomplex of Sec15p and Sec10p is localized to secretory vesicles (2) and a network of protein-protein interactions among the exocyst components bridges Sec15p-Sec10p to the targeting patch made by Sec3p (3).

In mammals the exocyst is involved in the targeting of Golgi-derived vesicles to the basolateral membrane of polarized epithelia. The regulation of the exocyst seems to be somewhat different in higher eukaryotes, because Sec3 does not have the same role. Rather, in polarized epithelial cells, Exo70 is localized to the plasma membrane (4), whereas the other components of the exocyst remain cytosolic, implying that exocyst assembly at the membrane is dependent upon Exo70, rather than Sec3 as in yeast.

Small GTPases of the Ras superfamily are involved in the regulation of a variety of cellular processes, including growth, differentiation, actin cytoskeleton, nuclear transport, and vesicle transport. Because many of these processes involve exocytosis, it was likely that small GTPases could play a role in exocyst regulation (5). In yeast, Sec4p, a homologue of Rab3A GTPase, anchors Sec15p to secretory vesicles (2). The exocyst is anchored to the plasma membrane via the interaction of Sec3p with another GTPase, Rho1p (6). Sec3p has also been shown to bind to Cdc42, another member of the Rho family (7). Finally, it was shown that Exo70p interacts with Rho3p at the plasma membrane (8). The role of the Rho family GTPases, which regulate the actin cytoskeleton, in exocyst regulation implies a coordination of cytoskeletal changes with exocytosis.

In mammalian cells, the exocyst components do not seem to interact with Rab3A or Rho family members. Rather, it was recently shown that the exocyst is regulated by yet another GTPase, RalA (9–12). Ral is a Ras family small G protein that is not present in *S. cerevisiae*. Both activated Ral and Ral inhibition disrupt polarized exocytosis in epithelial cells, suggesting it is necessary for the GTPase to cycle between the GDP- and GTP-bound forms to direct vesicle movement. Ral, like Rab3A, is localized to secretory vesicles and the plasma membrane, but the exocyst component responsible for interacting with RalA was found to be Sec5. In yeast, Sec5p is at the center of the exocyst complex, linking the Sec10p-Sec15p subcomplex to the rest of the exocyst via its interactions with Exo70p, Sec3p, and Sec6p (3). Thus, Sec5 may have a different role in the mammalian exocyst.

Ral small GTPases are members of the Ras superfamily of small G proteins implicated in oncogenesis, endocytosis, actin dynamics, and membrane trafficking. Downstream effector

\* This work was supported by Cancer Research UK and the European Commission. This work is a contribution from the Cambridge Centre for Molecular Recognition, which is supported by the Biotechnology and Biological Sciences Research Council and the Wellcome Trust. The costs of publication of this article were defrayed in part by the payment of page charges. This article must therefore be hereby marked "advertisement" in accordance with 18 U.S.C. Section 1734 solely to indicate this fact.

The atomic coordinates and structure factors (code 1hk6) have been deposited in the Protein Data Bank, Research Collaboratory for Structural Bioinformatics, Rutgers University, New Brunswick, NJ (<http://www.rcsb.org/>).

<sup>‡</sup> A Medical Research Council Career Development Fellow. To whom correspondence may be addressed. Tel.: 44-1223-766018; Fax: 44-1223-766002; E-mail: mott@bioc.cam.ac.uk.

<sup>¶</sup> Present address: Harvard Medical School, Massachusetts General Hospital Cancer Center, Bldg. 149, 13th St., Charlestown, MA 02129.

\*\* To whom correspondence may be addressed. Tel.: 44-1223-766018; Fax: 44-1223-766002; E-mail: do@bioc.cam.ac.uk.

proteins identified for Ral include Ral BP1<sup>1</sup> (or RLIP-76), which mediates the effects of Ral on endocytosis (13, 14) and interactions with the Rho family GTPases (15), filamin, an actin filament cross-linking protein, and phospholipase D1, which is involved in vesicle trafficking (16). The discovery that Ral is involved in regulation of exocytosis provides a link between secretory and cytoskeletal pathways.

The exocyst was found to bind specifically to GTP-bound RalA (11). One region of small G proteins that is sensitive to the state of the bound nucleotide is the effector loop, which interacts with downstream effectors. The effector loop mutant D49E does not bind to Sec5 and has been shown to disrupt transport of proteins to the basolateral surface in polarized epithelial cells (9).

The region of Sec5 responsible for Ral binding was identified and comprises the first 80 amino acids (10). The first 95 residues of Sec5 contain a putative domain, the IPT (17), which is found in some cell-surface receptors such as Met and Ron and in intracellular transcription factors, *e.g.* NF- $\kappa$ B, where it is responsible for DNA binding. A domain of this type has not been found in a G protein effector so far, and it is not possible to predict how it will interact with Ral. In contrast, the topology of the Ras-binding domain of the Ras effectors is structurally conserved and forms a ubiquitin-like fold (18, 48, 49). It is thus of great interest to study how the Ral GTPases (the closest homologues of Ras) interact with their own effectors. There is some precedent for Ig domain-G protein interactions. A guanine nucleotide dissociation inhibitor (GDI) for Rho family proteins contains an Ig domain, whose structure in complex with Cdc42 and Rac has been solved (19–21).

We have solved the structure of the Ral-binding domain of Sec5 using solution NMR techniques and find that it forms an IPT fold. We have mapped the binding of Ral-GMPPNP to this domain and found that the surface of Sec5 that interacts with Ral is similar to that used in other IPT domains for protein-protein interactions. Furthermore, this surface is different from that used in the Rho GDI Ig domain for contacting the Rho family proteins and their geranyl-geranyl moiety. How Ral may bind to the IPT domain of Sec5 will be discussed and compared with other G protein-effector interactions.

#### EXPERIMENTAL PROCEDURES

**Protein Expression**—The IPT domain of murine Sec5 (residues 5–97) was expressed as a His-tagged fusion protein. Labeled protein was produced by growing *Escherichia coli* BL21 in a medium based on MOPS buffer, containing 5% Celtone (Spectra Stable Isotopes), and <sup>15</sup>NH<sub>4</sub>Cl and/or <sup>13</sup>C<sub>6</sub>-glucose. The fusion protein was affinity purified on a Ni<sup>2+</sup> column and cleaved from its His-tag with Factor Xa (Roche) followed by gel filtration. The NMR buffer was 20 mM sodium phosphate, pH 6.0, 50 mM NaCl, 10 mM d<sub>10</sub>-dithiothreitol, 0.05% NaN<sub>3</sub>. NMR experiments were run with a protein concentration of ~1 mM.

Ral was expressed as a His-tagged fusion protein and affinity purified in the same manner as Sec5. The purified protein was concentrated and the bound nucleotide exchanged for the non-hydrolyzable GTP analogue, GMPPNP (Sigma) as described previously (22).

**NMR Spectroscopy**—NMR spectra were recorded at 25 °C on a Bruker DRX600 spectrometer, except for <sup>13</sup>C- and <sup>15</sup>N-separated NOESY experiments, which were recorded on a Bruker DRX800. The following experiments were recorded: <sup>15</sup>N HSQC; <sup>15</sup>N-separated NOESY (100 ms mixing time); <sup>15</sup>N-separated TOCSY (36 ms DIPSI-2 mixing); intra-HNCA (23); HN(CO)CA; HNCACB; CBCA(CO)NH; HNCO; (H)CC(CO)NH; H(CC)(CO)NH; HCCH-TOCSY (18 ms FLOPSY-16 mixing); <sup>13</sup>C HSQC; and <sup>13</sup>C-separated NOESY (100 ms

mixing time) (see Ref. 24 and references therein). Backbone torsion angles were estimated from CA, CO, CB, N, and HA chemical shifts using the program TALOS (25). NMR data were processed using the AZARA package and analyzed using ANSIG (26).

**Structure Calculation**—Structures were calculated iteratively, using CNS 1.0 and ARIA 1.0 (27). The parameters used for the calculation were essentially those described in Ref. 27 except that the length of the high temperature dynamics was increased to 45 ps and the cooling to a total of 39 ps. The  $\phi$  and  $\psi$  restraints from TALOS were included with errors of  $\pm 30^\circ$  or twice the S.D., whichever was greater.

**NMR Titration**—The buffer for the titration was 20 mM Tris-HCl, pH 7.5, 150 mM NaCl, 1 mM MgCl<sub>2</sub>, 0.05% NaN<sub>3</sub>. A 0.4-mM sample was prepared and used to record the first <sup>15</sup>N HSQC in the Ral titration. Ral-GMPPNP was then added into the Sec5 sample to give titration points at the following ratios; 1:0.1, 1:0.25, 1:0.38, 1:0.5, 1:0.8, 1:1, and 1:1.5 (Sec5:Ral-GMPPNP). <sup>15</sup>N HSQC spectra were recorded for each titration point.

#### RESULTS

**Description of the Structure**—Backbone resonances of the Sec5 IPT domain were assigned using intra-HNCA (23), HN(CO)CA, HNCACB, and CBCA(CO)NH experiments (reviewed in Ref. 24). Side chain resonances were assigned using (H)C-C(CO)NH, H(CC)(CO)NH, and HCCH-TOCSY experiments. NOEs were measured from <sup>15</sup>N-separated NOESY (961 NOEs) and <sup>13</sup>C-separated NOESY (2,662 NOEs) experiments.

Initial structures were calculated using a total of 2,941 unique (non-degenerate) NOE restraints, (1,350 unambiguous and 1,591 ambiguous) and 42 pairs of dihedral restraints from TALOS. After 8 iterations, there were 2,052 unambiguous NOEs and 828 ambiguous NOEs. In the final iteration, 100 structures were calculated; the 25 with the lowest energy were selected for analysis.

The structure of the Sec5 IPT is well defined by the NMR data and has good covalent geometry (Table I). The family of structures and the closest structure to the mean are shown in Fig. 1. The domain forms an Ig-like  $\beta$ -sandwich, consisting of eight  $\beta$ -strands that pack together into two  $\beta$ -sheets. The topology of the Sec5 domain is shown in Fig. 2, along with the topology of an Ig V-type domain and that of the IPT domain of the transcription factor NF- $\kappa$ B. The first  $\beta$ -strand is split into two, a and a', connected by three residues that form a bulge centered around Pro-15. This is followed by strand b, which packs against strand a in an anti-parallel fashion and then strands c and c', which form the edge of the second  $\beta$ -sheet. The b-c loop is interrupted by a single turn of  $3_{10}$  helix. The c' strand is followed by strand d, which forms the edge of the first  $\beta$ -sheet, packing against strand e. This is followed by strands f and g, which complete the second  $\beta$ -sheet. The last strand is also split into two: g, which forms an anti-parallel connection with strand f and g', which forms a parallel connection with strand a'.

**Comparison to Other IPT Domains**—The first structures of IPT domains determined were of the DNA-binding domains of transcription factors such as NF- $\kappa$ B (28, 29) and revealed a 7-stranded  $\beta$ -sandwich, which differs from that of the Ig V-type domains in that it is missing strand c' from the first  $\beta$ -sheet and strand d is much shorter (Figs. 2, b and c, and 3). A sequence alignment of Sec5 IPT with other IPT domains (Fig. 4) was constructed after the structure of Sec5 IPT was solved, on the basis of tertiary structure alignment of Sec5 with NF- $\kappa$ B (28) and *Bacillus stearothermophilus*  $\alpha$ -amylase (30) (PDB codes 1bfs and 1qho), using TOP (31). Alignment on the basis of sequence alone was not accurate, even when the secondary structures of IPT domains such as NF- $\kappa$ B were used to guide the alignment. The sequence alignment available from data bases such as Pfam is also incompatible with this structure-based alignment, probably because the sequence identity between Sec5 and the other IPT domains is extremely low.

<sup>1</sup> The abbreviations used are: Ral BP1, Ral-binding protein 1; Ig, immunoglobulin; IPT, Ig-like, plexins, transcription factors; GDI, guanine nucleotide dissociation inhibitor; NMR, nuclear magnetic resonance; HSQC, heteronuclear single quantum correlation; NOESY, nuclear Overhauser effect spectroscopy; TOCSY, total correlation spectroscopy; MOPS, 3-(*N*-morpholino)propanesulfonic acid.

TABLE I  
Experimental restraints and structural statistics

Number of experimental restraints		
Unambiguous	2052	
Ambiguous	828	
Dihedral restraints from Talos	84	
	$\langle SA \rangle^a$	$\langle SA \rangle_c^b$
Co-ordinate precision		
r.m.s.d. <sup>c</sup> of backbone atoms (7–94) (Å)	$0.55 \pm 0.07$	0.44
r.m.s.d. of all heavy atoms (7–94) (Å)	$0.94 \pm 0.12$	0.82
r.m.s.d.		
From the experimental restraints		
NOE distances (Å)	$0.009 \pm 0.002$	0.008
Talos dihedral angles (°)	$0.317 \pm 0.051$	0.271
From idealized geometry		
Bonds (Å)	$0.0015 \pm 0.00009$	0.0015
Angles (°)	$0.321 \pm 0.007$	0.315
Impropers (°)	$0.202 \pm 0.013$	0.215
Final energy		
$E_L - J^d$ (kcal/mol)	$-669.34 \pm 7.93$	-671.67
Ramachandran analysis		
Residues in most favored region	70.4%	72.0%
Residues in additionally allowed region	21.1%	20.0%
Residues in generously allowed regions	8.5%	8.0%
Residues in disallowed regions	0.0%	0.0%

<sup>a</sup>  $\langle SA \rangle$  represents the average r.m.s. deviations for the ensemble.

<sup>b</sup>  $\langle SA \rangle_c$  represents values for the structure that is closest to the mean.

<sup>c</sup> r.m.s.d., root mean square deviations.

<sup>d</sup> The Lennard-Jones potential was not used at any stage in the refinement.

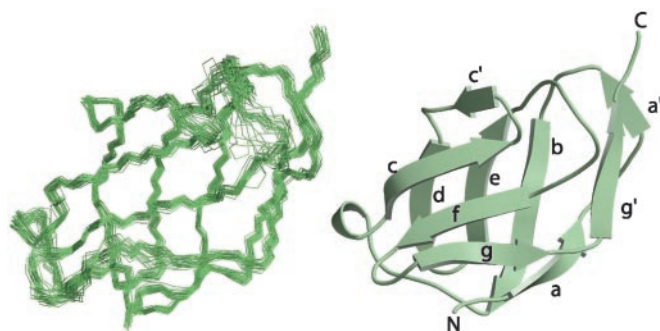


FIG. 1. The structure of the Sec5 IPT domain. On the left is a backbone trace of the 25 lowest energy structures. On the right is a ribbon representation of the structure that is closest to the mean. The  $\beta$ -strands are labeled. This figure was generated with Molscript (45) and Raster3D (46).

The transcription factor IPT domains have two major roles; they are involved in DNA binding and homo- and heterodimerization. The IPT domains whose structures have been solved by x-ray crystallography in complex with either DNA, another IPT domain, or other protein domains were analyzed using the program CONTACT (32) with a cutoff distance of 4.0 Å. The residues involved in DNA binding are generally basic or polar (Fig. 4, shaded blue) and are not conserved in IPT domains that do not interact with nucleic acids, such as  $\alpha$ -amylase and Sec5. The IPT domains are also involved in contacting other protein domains within the same molecule. Although the residues are not likely to be conserved between different proteins, they highlight regions of the IPT domain that may generally be involved in protein-protein interactions (Fig. 4, shaded green). They include the a'/g' surface (Figs. 3 and 4) and the b/e surface in both  $\alpha$ -amylase and the transcription factors.

**Delineation of the Ral Binding Site**—The Sec5 IPT domain binds to Ral, and the binding contacts on Sec5 were mapped by titrating unlabeled Ral into <sup>15</sup>N-labeled Sec5. The resulting changes in the <sup>15</sup>N HSQC spectrum are shown in Fig. 5A. When two proteins interact, the chemical environment of the backbone amides changes, and this usually causes a change in chemical shift. Such changes can be grouped into three regimes: fast, intermediate, and slow. The regime observed for

any amide depends on the relationship between the chemical shift difference and the rate of exchange between the free and bound states. If the exchange rate were higher than the chemical shift difference, a single peak would appear at a position between the chemical shift of the free and bound forms. If the exchange rate is lower than the chemical shift difference, two peaks would be observed, one for the free form and one for the bound. In the intermediate case (the exchange rate is comparable with the chemical shift difference), the peaks become broadened and may be unobservable. In the Sec5-Ral complex spectra, all the resonances that change significantly are in slow or intermediate exchange. None of the resonances appear to be in fast exchange, because they do not shift gradually as more G protein is added (Fig. 5A). In addition, new resonances appear as the ratio of Sec5:Ral approaches 1:1, for example that of Leu-92 (Fig. 5A). There is a trend for the signal intensities to decrease because of the increase in correlation time between 10 kDa Sec5 and the 30 kDa Sec5-Ral complex. Some resonances in Sec5 disappear completely in the 1:1 complex, e.g. Arg-37 (Figs. 4 and 5A). It should be noted that NMR mapping implicates a larger surface than the actual contact site, because secondary effects will be observed. Thus, changes in backbone amides that are not exposed to the solvent have been excluded from Figs. 3 and 5B. In Sec5, the changes are concentrated on one face of the domain, comprising strands a, b, e, and g (Figs. 2, 3, and 5B). There are no changes in strands c, c', and f.

#### DISCUSSION

The structural and sequence alignments reveal that, although the overall folds are similar, the Sec5 domain is more similar to the bacterial  $\alpha$ -amylases than to NF- $\kappa$ B (Figs. 3 and 4). One of the major differences between these domains is the region between strands c and e. In NF- $\kappa$ B there is a loop containing a single turn of a  $3_{10}$  helix, then the c' strand, then another turn of  $3_{10}$  helix and strand d, which is only 2 residues; in Sec5 and  $\alpha$ -amylase the loop between c and c' is much shorter and does not contain any helix and strand d is longer (Fig. 4). The other main difference between Sec5/ $\alpha$ -amylase and the transcription factors is that there is a 6-residue insertion in the e-f loop in the DNA-binding proteins. This insertion is visible in the structures, because the loop protrudes from the surface in NF- $\kappa$ B (Fig. 3).

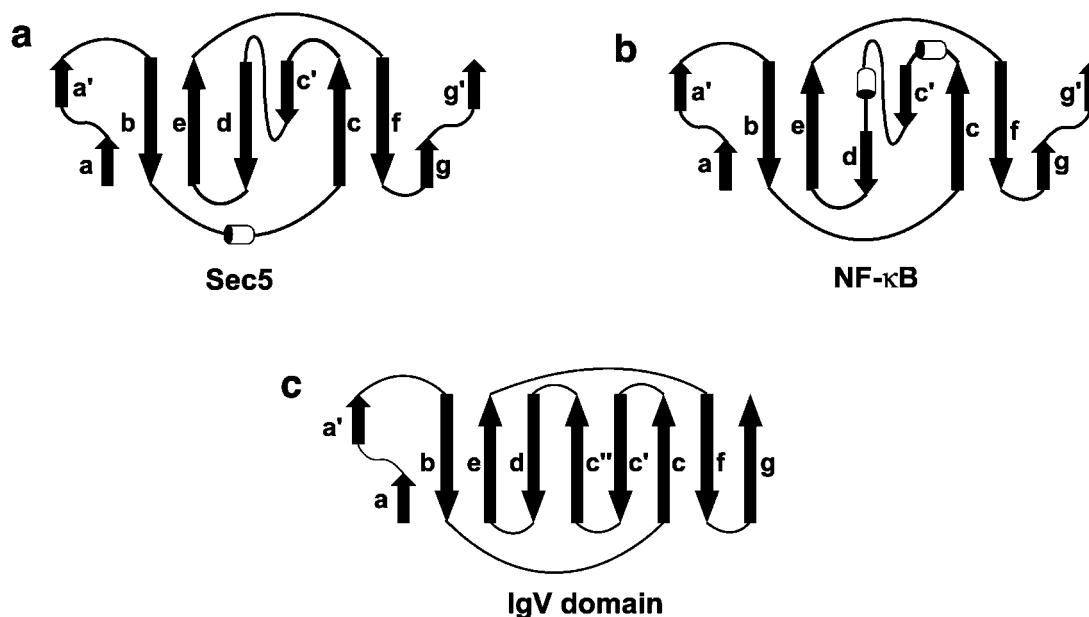


FIG. 2. **Topologies of Ig-like domains.** The topology of the Sec5 IPT domain (a), the NF- $\kappa$ B transcription factor IPT domain (b), and the Ig V-type domain (c). Although the cores of the two  $\beta$ -sheets are the same in all the domains, the strands at the edges of the sheets are different and in the IPT domains there are variable short stretches of  $3_{10}$  helix within the inter-strand loops.



FIG. 3. **Comparison of the structures of Sec5 with other IPT domains and Rho GDI.** The  $\beta$ -strands are labeled in the Sec5 domain. The e-f loop, the site of an insertion in NF- $\kappa$ B, is labeled.

The residues involved in dimerization in the transcription factors map to one surface of the domain, comprising residues from  $\beta$ -strands a, b, d, and e (Figs. 4 and 5B, shown in red). This is in contrast to Ig-Ig interactions, such as the Cd2-Cd58 complex, where the interaction surface is on the opposite surface of the  $\beta$ -sandwich and is composed of residues in strands g, f, c, and c' (33). The residues involved in dimerization are generally hydrophobic, although some salt bridges are also found in the dimer interfaces. These hydrophobic residues are not conserved in Sec5 except where they are involved in packing (e.g. Ile-13). There is one notable exception, Val-61 in Sec5, which is not conserved in  $\alpha$ -amylase and is equivalent to Val-313 in NF- $\kappa$ B. This side chain is exposed on the surface of the Sec5 even

though it is hydrophobic. Despite this, it is not likely that Sec5 dimerizes via the IPT domain in a manner similar to the transcription factors; the correlation time of this domain, determined from the T1/T2 ratios of residues in secondary structure, is 5.9 ns (data not shown), which is consistent with a monomeric protein of this size.

The Ral binding surface on the Sec5 IPT domain can be compared with the regions of the IPT domains involved in interactions with other molecules (Figs. 4 and 5B, shown in green). The  $\alpha$ -amylase IPT domain uses the same face to contact other domains within the same protein (30). NF- $\kappa$ B and the other DNA-binding proteins use the same face both for contacting other IPT domains and for contacting other domains within the same protein (28, 29, 34–40). The DNA-binding residues in these IPT domains are close to the protein-protein interaction surface but only partially overlap. Interestingly, the other Ig-like domain that has been found to contact G proteins, that from Rho GDI, uses the opposite face to contact the Rho family proteins (Fig. 5B) (19–21). It is perhaps not surprising that this divergence in binding interfaces exists between the GDI and Sec5, because the GDI domain is quite different; it has several extra  $\beta$ -strands, one of which is involved in G protein binding (Figs. 3 and 5B). In addition, the GDI domain, although it interacts with the G protein, makes the majority of its contacts with the geranyl-geranyl moiety that is covalently attached to the C terminus of the Rho family proteins.

A number of G protein-effector complex structures have been solved and have shown that the way that proteins can contact G proteins varies significantly. In most G protein-effector complexes, the effector contacts switch I (the effector loop). The Sec5 domain also makes contacts with the effector loop, because mutation of Asp-49 of Ral abrogates its interaction with Sec5 (9). In other G protein-effector complexes, the structural motifs that interact with the effector loop vary widely, so it is not possible to predict which region of Sec5 may be contacting this region of Ral.

In several complexes, for example the Ras-effector complexes (18, 48, 49) and the Cdc42-CRIB effector complexes (41, 50, 51), an intermolecular  $\beta$ -sheet is observed, formed by an interaction

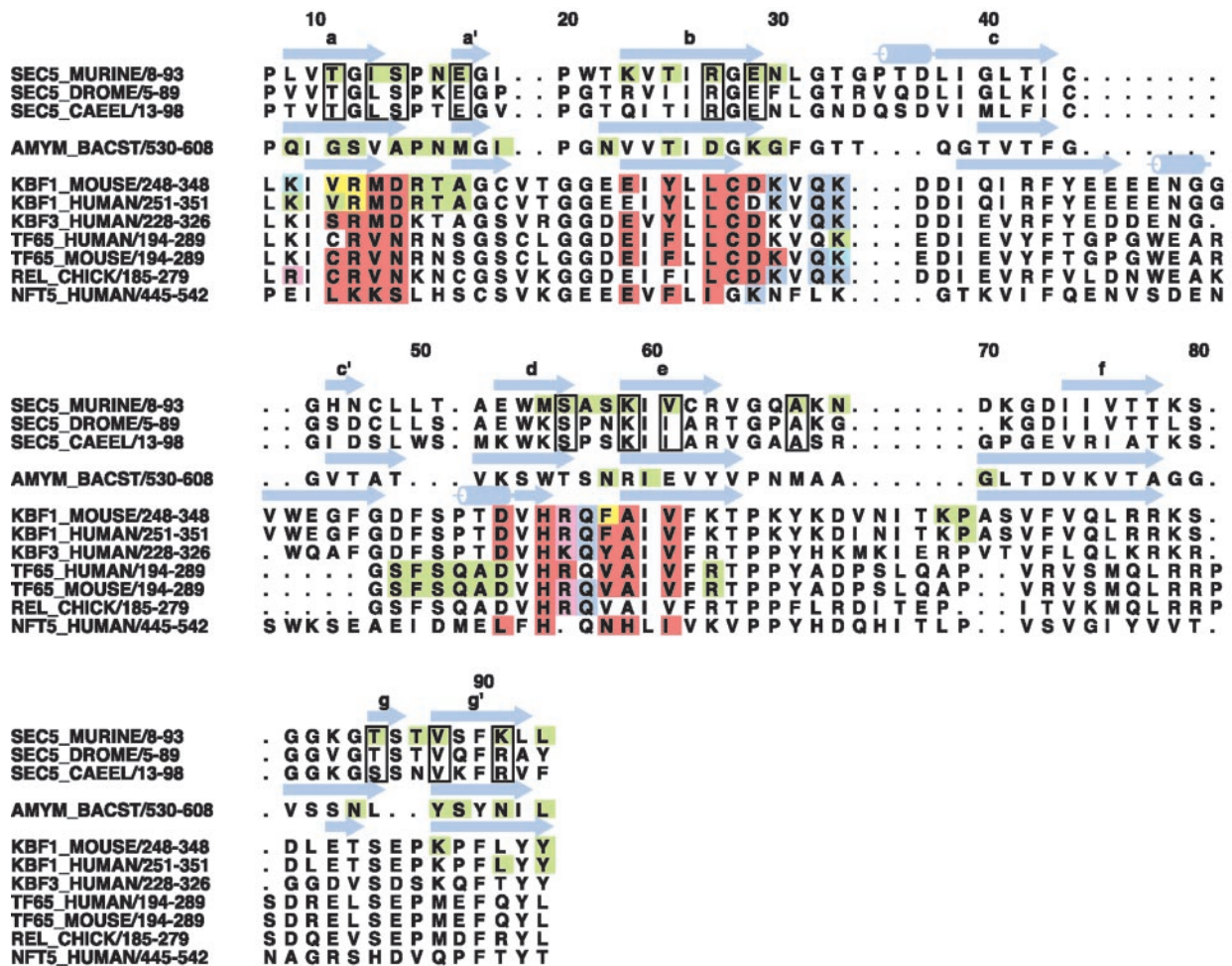


FIG. 4. Sequence alignment of IPT domains whose structures have been determined with the Sec5 IPT domains from various organisms. The murine Sec5 IPT domain is identical to that of human Sec5. The residue numbers for murine Sec5 are shown above the sequences. The basis of this alignment was taken from Pfam, but Sec5 was added by using an alignment of the three-dimensional structure with that of  $\alpha$ -amylase and mouse NF- $\kappa$ B p50. The secondary structures of these three proteins are shown in blue above the sequences, with cylinders representing  $\alpha$ -helices and arrows representing  $\beta$ -strands. The solvent-exposed residues in murine Sec5 that shift when Ral is added are colored green and are boxed if they are conserved between species. The other IPT domain residues involved in interacting with other molecules are colored as follows: DNA interactions, blue; dimer interface, red; interactions with other proteins or other domains, green; interactions with DNA and other proteins, cyan; dimer interface and interactions with DNA, magenta; dimer interface and interaction with other proteins, yellow. This figure was produced with Alscript (47).

between the  $\beta$ 2-strand of the G protein and a strand from the effector. In the case of Sec5, it is tempting to speculate that a similar intermolecular  $\beta$ -sheet will be formed in this effector complex, because many of the residues implicated in binding to the Ral are within strands a, b, e, and g. If an intermolecular  $\beta$ -sheet is formed in this complex, it must involve a  $\beta$ -strand of the Sec5 IPT that is available to make hydrogen bonds. The  $\beta$ -strand that fulfils this criterion and experiences chemical shift changes on Ral binding is strand d. If, however, this were involved in an intermolecular  $\beta$ -sheet interaction, there would have to be some structural rearrangement of the Sec5 because there is not enough space between strand d and the single turn of helix in the b-c loop to insert part of the G protein there.

The other Ral effector that has been studied in some detail is Ral BP1 or RLIP. The Ral-binding domain of this protein has been delineated and comprises residues 403–499 (15). Although there is no structure available for this protein, secondary structure predictions show that RLIP is predominantly  $\alpha$ -helix and that the Ral-binding domain partially overlaps a potential coiled-coil region. Thus, the interaction between Ral and RLIP is likely to be significantly different from that between Ral and Sec5. There are other G protein-effector complexes where the effector domain is predominantly  $\alpha$ -helix, e.g.

Rho-PKN (42), Rac-Arfaptin (43), and Rab-Rabphilin (44), but the structures and interactions are highly variable.

Although the IPT fold exists in most phyla, the IPT domain of Sec5 seems to appear with Ral in evolution. In *S. cerevisiae* and *Arabidopsis thaliana*, where Ral does not exist, Sec5 lacks the IPT. In *S. cerevisiae* the exocyst components that bind to G proteins do not contain any regions with homology to the IPT domains, so it is possible that Ral is the only small GTPase controlling the exocyst that binds an IPT. The other Ral effector proteins, Ral BP1, filamin, and phospholipase D, do not contain an IPT domain. It remains to be seen whether other Ral effectors are isolated that use an IPT to mediate their interaction with Ral.

Directed exocytosis is crucial to the regulation of several cellular processes. Central to the understanding of regulation of exocytosis is the role of small G proteins in recruitment of the components of the exocyst complex. We have solved the structure of the Ral-binding domain of the mammalian exocyst protein, Sec5. This is the first structure of a Ral effector domain and the first G protein effector that utilizes an IPT fold to contact the GTPase. We have shown that the Sec5 Ral-binding domain forms an IPT domain that is topologically closer to  $\alpha$ -amylase than to the transcription factors such as NF- $\kappa$ B.

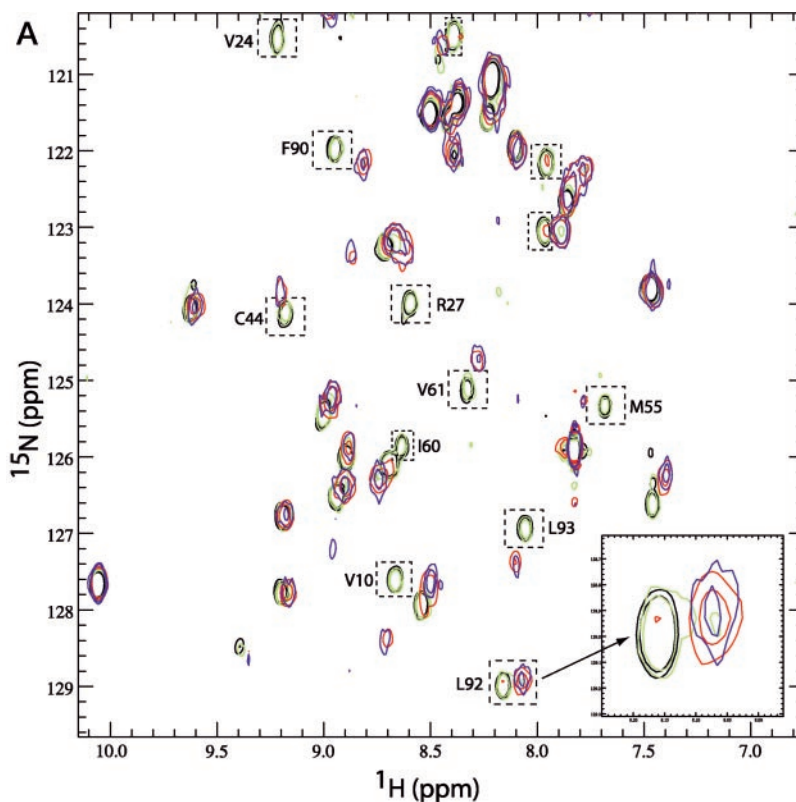
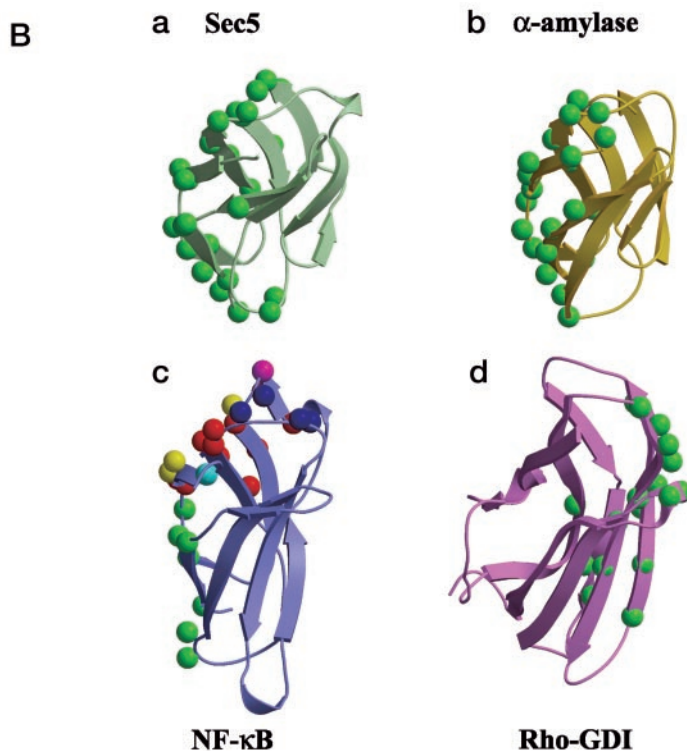


FIG. 5. *A*, the Sec5-Ral NMR titration. A section of the  $^{15}\text{N}$  HSQC is shown at three points in the titration as follows: *black* contours 1:0; *green* contours 1:0.5; *red* contours 1:1.0; *blue* contours 1:1.5. In each case the ratios denote Sec5: Ral-GMPPNP. Resonances that are in slow exchange are marked with a *dashed box*. An expansion is shown for the backbone amide of Leu-92; as the titration proceeds, the intensity of the peak on the *left* decreases until the final point when it has disappeared. At the same time, the intensity of the peak on the *right* increases. *B*, interaction surfaces in the IPT and GDI domains: Sec5 with Ral (*a*);  $\alpha$ -amylase with domains in the rest of the protein (*b*); NF- $\kappa$ B with DNA and other domains (*c*); Rho-GDI with Cdc42 (*d*). Location of residues involved in interactions with other molecules are denoted by *balls*, the color coding of which is the same as the shading of residues in Fig. 4.



Mapping of the Ral binding site in the Sec5 domain reveals that, within the family of IPT domains, a similar region is used for protein-protein interactions and that this region is not the same as that used for interacting with DNA. Comparison of the Ral-binding surface of Sec5 with the region of GDI that interacts with Rho family G proteins shows that the contacts between Sec5-Ral and GDI-Cdc42 are significantly different. A detailed analysis of the contacts that Sec5 makes with Ral

awaits determination of the three-dimensional structure of the complex. The information presented here can be used to help design mutants that disrupt Ral-Sec5 interactions. Such mutants could be used to elucidate the role of the Sec5-Ral interaction in exocyst assembly at the plasma membrane.

*Acknowledgment*—We thank Prof. Ernest Laue for constant support and encouragement.

## REFERENCES

1. Hsu, S. C., Hazuka, C. D., Foletti, D. L., and Scheller, R. H. (1999) *Trends Cell Biol.* **9**, 150–153
2. Guo, W., Roth, D., Walch-Solimena, C., and Novick, P. (1999) *EMBO J.* **18**, 1071–1080
3. Guo, W., Grant, A., and Novick, P. (1999) *J. Biol. Chem.* **274**, 23558–23564
4. Matern, H. T., Yeaman, C., Nelson, W. J., and Scheller, R. H. (2001) *Proc. Natl. Acad. Sci. U. S. A.* **98**, 9648–9653
5. Novick, P., and Guo, W. (2002) *Trends Cell Biol.* **12**, 247–249
6. Guo, W., Tamanoi, F., and Novick, P. (2001) *Nat. Cell Biol.* **3**, 353–360
7. Zhang, X. Y., Bi, E. F., Novick, P., Du, L. L., Kozminski, K. G., Lipschutz, J. H., and Guo, W. (2001) *J. Biol. Chem.* **276**, 46745–46750
8. Robinson, N. C. G., Guo, L., Imai, J., Toh-E, A., Matsui, Y., and Tamanoi, F. (1999) *Mol. Cell. Biol.* **19**, 3580–3587
9. Moskalenko, S., Henry, D. O., Rosse, C., Mirey, G., Camonis, J. H., and White, M. A. (2002) *Nat. Cell Biol.* **4**, 66–72
10. Sugihara, K., Asano, S., Tanaka, K., Iwamatsu, A., Okawa, K., and Ohta, Y. (2002) *Nat. Cell Biol.* **4**, 73–78
11. Brymora, A., Valova, V. A., Larsen, M. R., Roufogalis, B. D., and Robinson, P. J. (2001) *J. Biol. Chem.* **276**, 29792–29797
12. Polzin, A., Shipitsin, M., Goi, T., Feig, L. A., and Turner, T. J. (2002) *Mol. Cell. Biol.* **22**, 1714–1722
13. Jullien-Flores, V., Mahe, Y., Mirey, G., Leprince, C., Meunier-Bisceuil, B., Sorkin, A., and Camonis, J. H. (2000) *J. Cell Sci.* **113**, 2837–2844
14. Nakashima, S., Morinaka, K., Koyama, S., Ikeda, M., Kishida, M., Okawa, K., Iwamatsu, A., Kishida, S., and Kikuchi, A. (1999) *EMBO J.* **18**, 3629–3642
15. Jullienflores, V., Dorseuil, O., Romero, F., Letourneur, F., Saragosti, S., Berger, R., Tavitian, A., Gacon, G., and Camonis, J. H. (1995) *J. Biol. Chem.* **270**, 22473–22477
16. Luo, J. Q., Liu, X., Frankel, P., Rotunda, T., Ramos, M., Flom, J., Jiang, H., Feig, L. A., Morris, A. J., Kahn, R. A., and Foster, D. A. (1998) *Proc. Natl. Acad. Sci. U. S. A.* **95**, 3632–3637
17. Bork, P., Doerks, T., Springer, T. A., and Snel, B. (1999) *Trends Biochem. Sci.* **24**, 261–263
18. Nassar, M., Horn, G., Herrmann, C., Scherer, A., McCormick, F., and Wittinghofer, A. (1995) *Nature* **375**, 554–560
19. Hoffman, G. R., Nassar, N., and Cerione, R. A. (2000) *Cell* **100**, 345–356
20. Scheffzek, K., Stephan, I., Jensen, O. N., Illenberger, D., and Gierschik, P. (2000) *Nat. Struct. Biol.* **7**, 122–126
21. Gosser, Y. Q., Nomanbhoy, T. K., Aghazadeh, B., Manor, D., Combs, C., Cerione, R. A., and Rosen, M. K. (1997) *Nature* **387**, 814–819
22. Owen, D., Mott, H. R., Laue, E. D., and Lowe, P. N. (2000) *Biochemistry* **39**, 1243–1250
23. Nietlispach, D., Ito, Y., and Laue, E. D. (2002) *J. Am. Chem. Soc.* **124**, 11199–11207
24. Ferentz, A. E., and Wagner, G. (2000) *Q. Rev. Biophys.* **33**, 29–65
25. Cornilescu, G., Delaglio, F., and Bax, A. (1999) *J. Biomol. NMR* **13**, 289–302
26. Kraulis, P. J., Domaille, P. J., Campbell-Burk, S. L., Vanaken, T., and Laue, E. D. (1994) *Biochemistry* **33**, 3515–3531
27. Linge, J. P., O'Donoghue, S. I., and Nilges, M. (2001) **339**, 71–90
28. Ghosh, G., Vanduyne, G., Ghosh, S., and Sigler, P. B. (1995) *Nature* **373**, 303–310
29. Muller, C. W., Rey, F. A., Sodeoka, M., Verdine, G. L., and Harrison, S. C. (1995) *Nature* **373**, 311–317
30. Dauter, Z., Dauter, M., Brzozowski, A. M., Christensen, S., Borchert, T. V., Beier, L., Wilson, K. S., and Davies, G. J. (1999) *Biochemistry* **38**, 8385–8392
31. Lu, G. G. (2000) *J. Appl. Crystallogr.* **33**, 176–183
32. Bailey, S. (1994) *Acta Crystallogr. Sect. D Biol. Crystallogr.* **50**, 760–763
33. Wang, J., Smolyar, A., Tan, K. M., Liu, J., Kim, M. Y., Sun, Z. J., Wagner, G., and Reinherz, E. L. (1999) *Cell* **97**, 791–803
34. Chen, F. E., Huang, D. B., Chen, Y. Q., and Ghosh, G. (1998) *Nature* **391**, 410–413
35. Chen, Y. Q., Ghosh, S., and Ghosh, G. (1998) *Nat. Struct. Biol.* **5**, 67–73
36. Stroud, J. C., Lopez-Rodriguez, C., Rao, A., and Chen, L. (2002) *Nat. Struct. Biol.* **9**, 90–94
37. Chen, L., Glover, J. N. M., Hogan, P. G., Rao, A., and Harrison, S. C. (1998) *Nature* **392**, 42–48
38. Jacobs, M. D., and Harrison, S. C. (1998) *Cell* **95**, 749–758
39. Huxford, T., Huang, D. B., Malek, S., and Ghosh, G. (1998) *Cell* **95**, 759–770
40. Cramer, P., Larson, C. J., Verdine, G. L., and Muller, C. W. (1997) *EMBO J.* **16**, 7078–7090
41. Mott, H. R., Owen, D., Nietlispach, D., Lowe, P. N., Manser, E., Lim, L., and Laue, E. D. (1999) *Nature* **399**, 384–388
42. Maesaki, R., Ihara, K., Shimizu, T., Kuroda, S., Kaibuchi, K., and Hakoshima, T. (1999) *Mol. Cell.* **4**, 793–803
43. Tarricone, C., Xiao, B., Justin, N., Walker, P. A., Rittinger, K., Gamblin, S. J., and Smerdon, S. J. (2001) *Nature* **411**, 215–219
44. Ostermeier, C., and Brunger, A. T. (1999) *Cell* **96**, 363–374
45. Kraulis, P. J. (1991) *J. Appl. Crystallogr.* **24**, 946–950
46. Merritt, E. A., and Bacon, D. J. (1997) *Methods Enzymol.* **277**, 505–524
47. Barton, G. J. (1993) *Protein Eng.* **6**, 37–40
48. Vetter, I. R., Linnemann, T., Wohlgemuth, S., Geyer, M., Kalbitzer, H. R., Herrmann, C., and Wittinghofer, A. (1999) *FEBS Lett.* **451**, 175–180
49. Huang, L., Weng, X. W., Hofer, F., Martin, G. S., and Kim, S. H. (1997) *Nat. Struct. Biol.* **4**, 609–615
50. Abdul-Manan, N., Aghazadeh, B., Liu, G. A., Majumdar, A., Ouerfelli, O., Siminovitch, K. A., and Rosen, M. K. (1999) *Nature* **399**, 379–383
51. Morreale, A., Venkatesan, M., Mott, H. R., Owen, D., Nietlispach, D., Lowe, P. N., and Laue, E. D. (2000) *Nat. Struct. Biol.* **7**, 384–388

## Structure of the GTPase-binding Domain of Sec5 and Elucidation of its Ral Binding Site

Helen R. Mott, Daniel Nietlispach, Louise J. Hopkins, Gladys Mirey, Jacques H. Camonis and Darerca Owen

*J. Biol. Chem.* 2003, 278:17053-17059.

doi: 10.1074/jbc.M300155200 originally published online March 6, 2003

---

Access the most updated version of this article at doi: [10.1074/jbc.M300155200](https://doi.org/10.1074/jbc.M300155200)

Alerts:

- [When this article is cited](#)
- [When a correction for this article is posted](#)

[Click here](#) to choose from all of JBC's e-mail alerts

This article cites 50 references, 13 of which can be accessed free at <http://www.jbc.org/content/278/19/17053.full.html#ref-list-1>